

# 摩擦学学报

TRIBOLOGY



## 不同岩石工况下新型高硬韧TBM刀圈用钢的磨损特性试验研究

蒋金哲, 刘越, 刘春明

### Experimental Investigation on the Wear Characteristics of a Novel TBM Cutter Ring Material with High Hardness and High Toughness under Different Rock Conditions

JIANG Jinzhe, LIU Yue, LIU Chunming

在线阅读 View online: <https://doi.org/10.16078/j.tribology.2023029>

#### 您可能感兴趣的其他文章

Articles you may be interested in

##### 新型TBM刀圈材料微观组织及耐磨性能研究

Microstructure and Wear Resistance of Novel TBM Cutter Ring Steel

摩擦学学报. 2021, 41(1): 17 <https://doi.org/10.16078/j.tribology.2020051>

##### 利用圆锥压头微米划痕测试材料断裂韧性

Fracture Toughness Measurement by Micro-Scratch Tests with Conical Indenter

摩擦学学报. 2019, 39(5): 556 <https://doi.org/10.16078/j.tribology.2019021>

##### 干气密封推环用弹簧蓄能密封圈工作特性研究

Working Performance of Push Ring's Spring Energized Seal

摩擦学学报. 2021, 41(4): 532 <https://doi.org/10.16078/j.tribology.2020152>

##### 恒定大载荷划痕试验下紫铜的三维形貌及划痕硬度分析

Analysis of 3D Morphology and Scratch Hardness of Copper under Large Constant Load

摩擦学学报. 2021, 41(4): 467 <https://doi.org/10.16078/j.tribology.2020140>

##### 18Ni(300)钢高速干滑动摩擦磨损特性研究

Friction and Wear Characteristics of 18Ni(300) Steel at High Speed Dry Sliding Condition

摩擦学学报. 2017, 37(2): 218 <https://doi.org/10.16078/j.tribology.2017.02.011>



关注微信公众号, 获得更多资讯信息

蒋金哲, 刘越, 刘春明. 不同岩石工况下新型高硬韧TBM刀圈用钢的磨损特性试验研究[J]. 摩擦学学报(中英文), 2024, 44(5): 622–632. JIANG Jinzhe, LIU Yue, LIU Chunming. Experimental Investigation on the Wear Characteristics of a Novel TBM Cutter Ring Material with High Hardness and High Toughness under Different Rock Conditions[J]. Tribology, 2024, 44(5): 622–632. DOI: 10.16078/j.tribology.2023029

## 不同岩石工况下新型高硬韧TBM 刀圈用钢的磨损特性试验研究

蒋金哲, 刘越\*, 刘春明\*

(东北大学材料科学与工程学院, 辽宁沈阳 110819)

**摘要:** TBM刀圈的磨损性能不仅取决于刀圈自身的组织及性能, 而且与岩石的类型以及磨损载荷紧密相关. 为此, 选取了5种不同性能的刀圈钢, 研究了磨损载荷以及岩石类型对试验钢磨损性能及磨损机制的影响. 研究结果表明: 在砂岩工况下, 不同性能试验钢均表现出微观切削磨损机制, 随着试验钢硬度的增加, 磨损量减小, 磨屑由卷曲条带状转变为木屑状. 在花岗岩工况下, 各试验钢磨损机制以犁削为主, 磨屑呈粉末状或块状, 磨损载荷较低时, 耐磨性与试样硬度正相关, 当磨损载荷增加到一定数值后, 耐磨性同时取决于试验钢的硬度和韧性.

**关键词:** TBM刀圈; 硬度; 韧性; 磨损行为; 岩石类型

中图分类号: U455.3; TH117.1

文献标志码: A

文章编号: 1004-0595(2024)05-0622-11

## Experimental Investigation on the Wear Characteristics of a Novel TBM Cutter Ring Material with High Hardness and High Toughness under Different Rock Conditions

JIANG Jinzhe, LIU Yue\*, LIU Chunming\*

(School of Materials Science and Engineering, Northeastern University, Liaoning Shenyang 110819, China)

**Abstract:** The wear resistance of TBM cutter ring material not only depends on its own microstructure and mechanical properties, but also closely related to the type of rock and wear load. Under different wear conditions, the wear mechanism of experimental steel with different mechanical properties is quite different, which leads to great changes in the wear resistance. TBM cutter ring material belongs to high alloy martensitic steel, its microstructure is composed of tempered martensite and carbide. The carbide with high hardness can ensure good wear resistance, while the hardness and impact toughness of TBM cutter ring steel can be adjusted effectively by tempered martensite. The tempering temperature and holding time is the main means to adjust the characteristics of tempered martensite. In this paper, five kinds of experimental steels with varying hardness and impact toughness gradient were prepared by different tempering treatment. The variation rules of wear resistance of experimental steels with different properties were studied under different wear loads and different rock types, and the wear morphologies of the wear surface and subsurface were observed and analyzed by scanning electron microscopy. The evolution of wear mechanism of experimental steels with different properties under different wear conditions was revealed. Specifically, the wear behavior of cutter ring steel with different mechanical properties under different types of rocks in real production process was simulated. The results

Received 1 March 2023, revised 13 July 2023, accepted 17 July 2023, available online 8 August 2023.

\*Corresponding author. E-mail: dbdx555@163.com, Tel: +86-13940062930; E-mail: cmliu@mail.neu.edu.cn, Tel: +86-13609880333.

This project was supported by the National Natural Science Foundation of China (52101171).

国家自然科学基金项目(52101171)资助.

showed that under the wear condition of sandstone, the wear mechanism of test steel with different mechanical properties was microscopic cutting. With the increase of hardness, the mass loss of specimens decreased, and the wear debris changed from strip to sawdust. The greater the wear load, the higher the wear mass loss of the test steel. Under the wear condition of granite, the wear mechanism of each test steel was mainly micro-ploughing and the wear resistance was positively correlated with hardness when the wear load was lower than 3 kN, and no crack appeared on the worn surface of each test steel. Meanwhile, the wear debris were powdery or block. When the load increased to 5 000 N, crack gradually occurred on the worn surface of experimental steel with the increase of hardness. For the cutter ring steel with toughness higher than 8 J, the wear mechanism was mainly micro-ploughing. When the toughness of the test steel was lower than 7 J, cracks appeared the worn surface, which resulted in a sharp weakening of the wear resistance of test steel. Therefore, when the load was higher than 3 kN, the wear resistance of the experimental steel depended on both hardness and toughness, and the experimental steel with good hardness and toughness had better wear resistance. The research on the wear behavior of cutter ring steel with different mechanical properties under different rock types provided a theoretical basis for the selection of cutter ring properties in practical application.

**Key words:** TBM cutter ring; hardness; toughness; wear behavior; rock type

全断面隧道掘进机(TBM)广泛应用于地铁、公路、铁路、市政和水利水电等地下工程建设,对世界各国的现代化建设起到了极大的推动作用<sup>[1]</sup>. 中国TBM的发展可谓是困难重重,先后经历了国外封锁阶段、中外合资阶段和独立研发阶段<sup>[2]</sup>. 自2013中国进入TBM自主创新和对外出口以来,我国在TBM大型化和智能化设计方面做出了非常大的突破. 然而,我国在TBM核心部件的研发方面依然处于落后地位,特别是主轴承和刀圈方面. 刀圈好比TBM的牙齿,在TBM施工过程中负责碾压岩石,直接影响着TBM的掘进成本及效率. 大量的工程实践表明,更换刀圈的成本高达隧道建设总成本的20%,同时检查、更换或修理刀圈的过程会使隧道工程的完成时间增加30%,在挖掘坚硬的磨蚀性岩石时刀圈的消耗更加严重<sup>[3-5]</sup>. 因此,开发长寿命TBM刀圈材料对提高隧道施工效率和降低施工成本至关重要.

近些年来,相关学者在TBM刀圈材料的力学性能及耐磨性方面做了大量的研究. 南昌大学闫洪团队<sup>[6-9]</sup>研究了退火、淬火及回火热处理工艺对5Cr5MoSiV1钢刀圈组织性能的影响,通过对试验钢晶粒尺寸、马氏体固溶度、残余奥氏体以及析出相随热处理工艺的变化研究,优化出了较为合适的热处理工艺参数. 吉林大学赵宏伟团队<sup>[10]</sup>对国内外生产的H13钢刀圈成分、硬度、冲击韧性和弹性模量等性能进行了详细的对比分析,结果表明国产刀圈在硬度上已经和进口刀圈相接近,但在冲击韧性上远低于德国Wirth刀圈,发现向H13刀圈钢中添加一定量的Ni元素可以提高残余奥氏体含量,进而提升冲击韧性. 燕山大学孙建亮团队<sup>[11]</sup>对国内外常用刀圈进行了解剖试验,从钢的纯净度、

冲击韧性、硬度及显微组织等方面对国内外刀圈进行了对比分析,另外其团队采用模锻和超细化热处理制备的刀圈性能达到了国外水平. 除了刀圈组织性能研究外,学者们对刀圈的磨粒磨损行为也进行了大量研究. 贾连辉等<sup>[12]</sup>采用橡胶轮磨损试验机研究了合金碳化物特征对H13钢刀圈磨损性能的影响,发现耐磨相的尺寸和形貌是影响刀圈钢耐磨性的主要因素,大块的共晶碳化物对耐磨性有非常大的提升作用. 中南大学夏毅敏团队<sup>[13-16]</sup>采用台架试验研究不同岩石类型、冷却速率以及干湿条件等一系列工况下H13钢刀圈的磨损量及磨损机理,发现刀圈的磨损并非越硬越耐磨,刀圈耐磨性还取决于地质条件及其刀圈材料的韧性. 邱涵等<sup>[17]</sup>发现在不同比例石英砂掺杂环境下,由于犁削行为的差异,低合金马氏体钢的磨料磨损性能存在明显的差异.

从目前刀圈材料的研究状况来看,关于新型TBM刀圈材料开发应用的报道相对较少,以往的研究多集中在传统的H13钢刀圈热处理及性能测试方面. 另外,关于刀圈材料磨损行为的研究存在一些不足,例如在橡胶轮磨损试验机磨损载荷较小,与真实工况下刀圈受到的磨损载荷差距较大,而台架试验虽然弥补了磨损载荷方面的缺点,但是对磨损过程中刀圈材料自身的组织性能变化研究不够深入.

在前期的工作中,作者针对刀圈微观组织与性能的关系做出了深入的研究,并依此开发出了TBM刀圈新材料<sup>[18-19]</sup>. 本研究中旨在采用超高应力磨损试验,研究不同硬度及韧性的新型TBM刀圈钢在不同岩石工况下的耐磨性,通过对磨损表面、磨损亚表面以及磨屑形貌的观察和分析,阐明在不同磨损工况下不同性

能刀圈的磨损失效机制. 研究结果为新型TBM刀圈的应用选型提供了理论依据.

## 1 试验部分

### 1.1 试验材料及制备方法

试验刀圈采用真空感应炉熔炼、氩气保护电渣重熔、多向锻造、辗环、机加工、退火以及淬火制备而成, 其化学成分列于表1中. 使用线切割沿圆周方向将

刀圈分切, 然后进行不同工艺的回火处理, 得到5种不同硬度与冲击韧性的刀圈试样, 为了便于表述, 将5种试验钢根据硬度从低到高依次命名为C1~C5, 各试验钢力学性能列于表2中. 5种试验钢的淬火工艺均为1 025 °C保温1.5 h后油淬, 回火热工艺分别为400 °C保温3 h空冷(C1试验钢), 450 °C保温3 h空冷(C2试验钢), 475 °C保温3 h空冷(C3试验钢), 475 °C保温12 h空冷(C4试验钢), 475 °C保温36 h空冷(C5试验钢).

表1 试验钢化学成分

Table 1 Chemical composition of experimental steel

Elements	C	Si	Mn	Cr	Mo	V	Ni	W	Nb	P	S
Mass fraction/%	0.85	0.90	0.43	6.76	1.82	0.30	0.85	0.35	0.25	0.005	0.02

表2 试验钢力学性能

Table 2 Mechanical properties of experimental steel

Samples	C1	C2	C3	C4	C5
Hardness/HRC	60.82	62.30	63.06	63.96	65.02
Impact toughness/J	13.40	9.59	8.49	8.11	6.94

选取TBM隧道施工过程中最为常见的砂岩和花岗岩作为摩擦对偶. 将每种岩石加工成直径50 mm, 高度100 mm的圆柱体, 采用MTS-H20型微机控制电液伺服压力试验机对试样进行压缩试验, 测得砂岩和花岗岩的抗压强度分别为80和200 MPa, 砂岩与花岗

岩的矿物成分列于表3中<sup>[20]</sup>. 从表3中可以看出, 2种岩石的成分均以方解石、长石和石英为主. 虽然砂岩抗压强度低, 但是砂岩富含大量细小的硬质石英颗粒. 花岗岩抗压强度高, 各种矿物相尺寸较大, 石英含量相对较低.

表3 岩石矿物成分

Table 3 Rock mineralogical compositions

Rock	Size/mm				Mass fraction/%			
	Quartz	Plagioclase	K-feldspar	Others	Quartz	Plagioclase	K-feldspar	Others
Sandstone	0.05~0.70	0.05~0.40	0.05~0.40	0.01~0.60	35	30	12	23
Granite	0.05~1.20	0.10~3.60	0.10~3.20	0.01~1.20	18	38	25	19

### 1.2 试验方案及表征方法

选用图1所示的MMU-10销-盘式磨损试验机进行磨损试验. 将试验钢加工成 $\Phi 5$  mm $\times$ 10 mm的圆柱体磨销. 将砂岩和花岗岩摩擦对偶都加工成 $\Phi 50$  mm $\times$ 60 mm的圆柱体. 磨损转速设置为100 r/min, 换算成线速度为12.56 m/min, 与实际工况下刀圈的旋转线速度相近. 实际工况下刀圈刃部不同位置处承受的压强不同, 刀刃顶部承受的压强最大, 需要超过岩石的抗压强度以碾碎岩石, 从刀刃顶端到两侧, 刀头受到的压强逐渐减小. 为了模拟实际工况下刀圈不同位置的磨损状况, 本次试验的磨损载荷选择1、3和5 kN, 换算成压强分别为50.95、152.87和254.77 MPa. 单次磨损时间

为1 h, 磨损过程中采用自来水对摩擦副进行冷却. 为了减小磨损试验误差, 将金属销棒进行打磨并抛光,

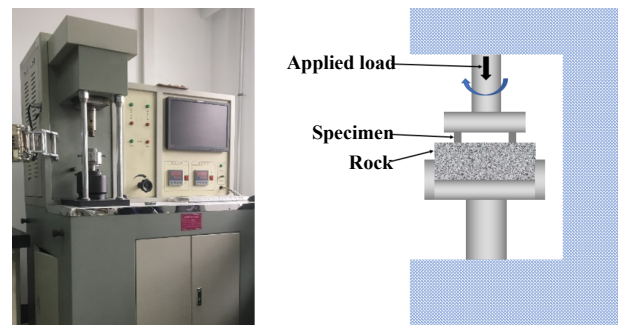


Fig. 1 MMU-10G friction and wear testing machine

图1 MMU-10G型摩擦磨损试验机

正式磨损前,先预磨5 min,然后用超声波清洗机清除磨损面岩石碎屑后用电子天平称重并记录,然后进行正式磨损试验.磨损测试结束后,将磨销取出,经过超声波清洗并干燥后称重并保存.每组磨损的试样重复测试3次,然后取3次磨损失重的平均值作为最终测试结果.

磨损测试结束后,使用场发射扫描电镜对各试验钢的磨损表面形貌、磨屑以及磨损亚表面进行观察分析,使用维氏硬度计对磨损亚表面的硬度分布进行测定.

## 2 结果与讨论

### 2.1 磨损失重

图2(a)和(b)所示分别为砂岩和花岗岩磨损工况下,C1~C5试验钢磨损失重随垂直载荷的变化.从图2中可以看出,无论与砂岩还是花岗岩相对摩擦时,不同性能试验钢的磨损失重均随着垂直载荷的增加而增大.相同磨损载荷和磨损时间下,相同性能的试验钢与砂岩磨损后的质量损失是与花岗岩磨损失重的数十倍,这与不同岩石的矿物成分及内部结构有关.

在砂岩磨损工况下,磨损载荷固定不变时,各试验钢的磨损失重均随着硬度的增大而减小,即硬度越高耐磨性越强,这与Saha等<sup>[21]</sup>的研究结果相似.C1钢的硬度最低,当磨损载荷最大(5 kN)时,其磨损失重最大,达到了4.632 g.而硬度最高的C5钢在1 kN载荷下的磨损量最小,失重只有0.411 g.马氏体初始硬度越高,抵抗磨粒压入磨损表面的能力越强,磨粒对试验钢的切削或者犁削作用也就越弱,因此磨损量随马氏体硬度升高而减少.除了马氏体初始硬度外,垂直载荷对磨粒在磨损表面的压入深度有很大影响,垂直载荷越大,磨粒在磨损表面的嵌入深度越大,对试验钢的切削能力越强<sup>[22]</sup>,因此磨损失重随着垂直载荷的增

加而增大.由此可以看出,在砂岩磨损工况下,试验钢的磨损失重与其硬度负相关,与磨损载荷正相关.

在花岗岩磨损工况下,各试验钢的磨损失重同样随着垂直载荷的增加而增加,但是与各试样的初始硬度不完全呈单调关系.从图2(b)可以看出,当垂直载荷不超过3 kN时,随着试验钢硬度的增加,磨损失重逐渐降低,这与砂岩工况下各试样磨损失重的变化规律一致.当垂直载荷达到5 kN时,各试验钢的磨损失重随着硬度的增加先降低后升高,C3钢的磨损失重最小.由此得出,在与花岗岩相对摩擦时,试验钢的磨损失重并非完全随试样硬度增加单调减小,而是同时取决于磨损载荷、试验钢的硬度及冲击韧性.在较低的磨损载荷下,试验钢的磨损失重变化趋势与硬度负相关.在较高的磨损载荷下,试验钢的磨损失重同时受硬度和韧性的影响,具有良好硬度与韧性匹配的试验钢磨损失重最小,这与Zhang等<sup>[16]</sup>的研究结果相似.

### 2.2 磨损表面及磨屑

使用场发射扫描电镜(SEM)分别对各试验钢与砂岩和花岗岩磨损后的磨损表面形貌进行了观察,如图3和图4所示.从图3中可以看出,与砂岩磨损后,不同试验钢磨损表面均出现了大量切削沟槽,由此可判断试验钢与砂岩磨损时,磨损机制主要为微观切削.在与砂岩磨损过程中,砂岩中锋利的石英磨粒刺入试验钢磨损表面,并与试样钢发生相对滑动,从而在试验钢磨损表面划出一道道划痕.磨损载荷一定时,试验钢的基体硬度越低,磨粒嵌入试验钢的深度越大,从试验钢磨损表面切削下的金属越多.从图3(a~c)可以看出,随着磨损载荷的增加,磨损机制由微切削向微犁削转变.从图3(c)可以看出,5 kN垂直载荷下,C1钢磨损表面除了显微切削痕迹外,还出现了严重的犁沟变形,在沟槽两侧可以明显看出由塑性变形产生的

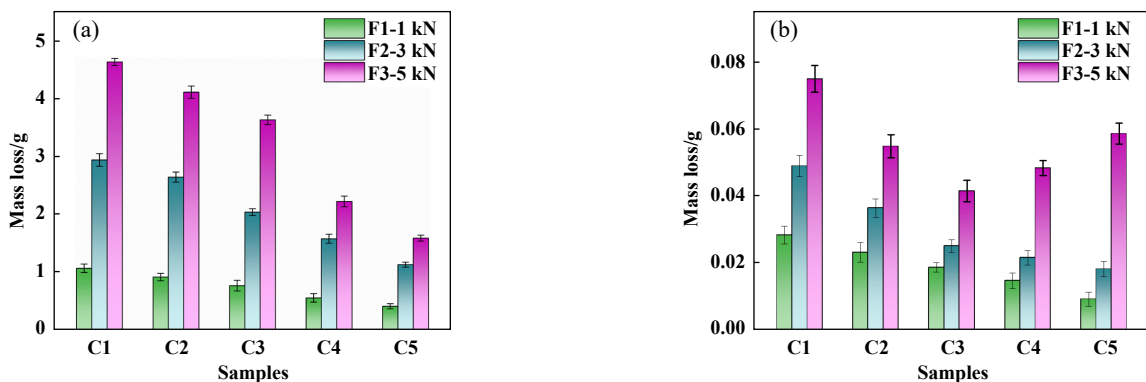


Fig. 2 Mass loss of each test steel under the wear condition of (a) sandstone and (b) granite

图2 (a)砂岩和(b)花岗岩磨损工况下各试验钢的磨损失重

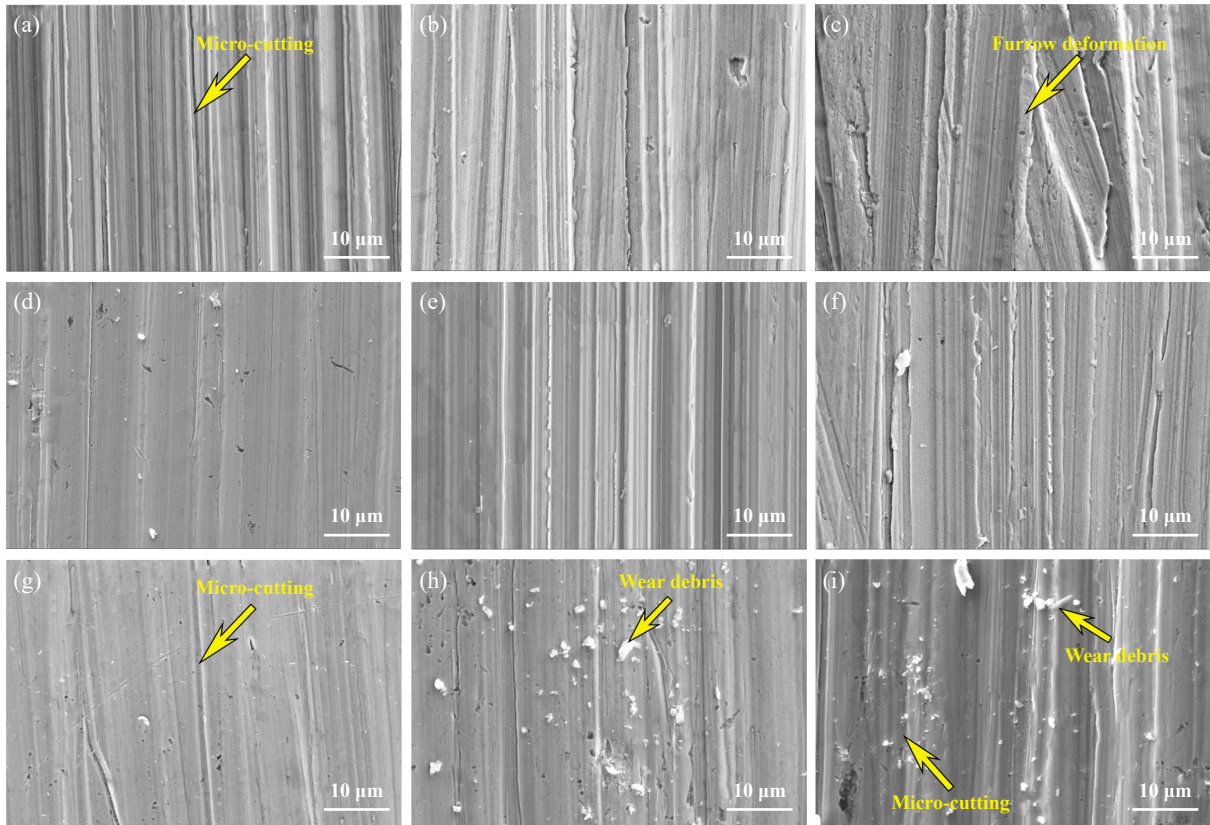


Fig. 3 SEM micrographs of worn surface morphology of experimental steels with different hardness after grinding with sandstone: (a) C1-1 kN; (b) C1-3 kN; (c) C1-5 kN; (d) C3-1 kN; (e) C3-3 kN; (f) C3-5 kN; (g) C5-1 kN; (h) C5-3 kN; (i) C5-5 kN

图3 与砂岩配副后不同硬度试验钢的磨损表面形貌的SEM照片

褶皱. 较高磨损载荷下, 塑性变形的产生与C1试验钢硬度较低而韧性较高有关. 相比于C1试验钢, C3试验钢磨损表面同样由大量的微切削沟槽组成, 但是在5 kN载荷下, C3试验钢磨损表面的塑性变形程度明显减弱, 说明提升试验钢的硬度有助于抵抗塑性变形. 从图4(g-i)可以看出, 硬度最高的C5钢磨损表面依然由大量的微切削沟槽构成, 但是相比C1和C3钢, C5钢磨损表面的切削沟槽宽度明显降低.

从图4可以看出, 与花岗岩相对摩擦后试验钢磨损表面由凿削坑和不同方向的划痕组成. 对于低硬度高韧性的C1钢, 磨损表面主要呈现出犁沟形貌, 随着磨损载荷的增加, 犁沟的宽度与深度也逐渐增加, 如图4(a-c)所示. 从图4(b)可以看出, 在犁沟中残存着团絮状的岩石碎屑, 在钢-岩相对滑动过程中, 岩屑推挤金属, 使之发生塑性流动, 进而犁出1条沟槽<sup>[23]</sup>. C3钢的磨损表面同样由犁沟组成[图4(d-f)], 但是相比硬度较低的C1钢, 犁沟的深度及宽度明显降低, 这与C3钢具有较高的硬度有关. 当磨损载荷低于3 kN时, 各试验钢的磨损表面均未出现裂纹, 并且随着试验钢硬度

的增加, 微切削沟槽的深度及宽度明显减小. 然而, 当磨损载荷达到5 kN时, 各试验钢的磨损表面形貌出现了明显差异, 硬度最高的C5钢磨损表面出现了大量裂纹, 硬度最低的C1钢磨损表面出现粗大的犁沟, 而硬度居中的C3钢的磨损表面仅由切削或犁削沟槽组成. 说明在与花岗岩高应力磨损过程中, 除了硬度外, 试验钢的韧性也对耐磨性起重要作用.

图5所示为各试样钢在不同载荷下与砂岩磨损后的磨屑形貌的SEM照片. 从图5(a-b)可以看出, C1试验钢磨屑呈卷曲的条带状, 磨损载荷为1 kN时, 磨屑条带宽度在5~15 μm之间, 当磨损载荷增加到5 kN时, 磨屑条带宽度在15 μm以上, 另外磨屑的卷曲程度明显增加. C1钢硬度低, 但是具有较高的韧性, 因此在磨损过程中, 尖锐的石英磨粒容易切入磨损表面, 产生厚度较大的磨屑, 同时磨屑韧性较好, 不容易发生断裂, 因此磨屑呈螺旋状. 相比C1钢, 在相同磨损条件下, C3钢的磨屑长度及卷曲程度明显低于C1钢, 如图5(c-d)所示. 这一方面是由于C3钢的硬度比C1钢高, 磨粒在C3试验钢磨损表面的切入深度较小, 因此磨屑宽度相

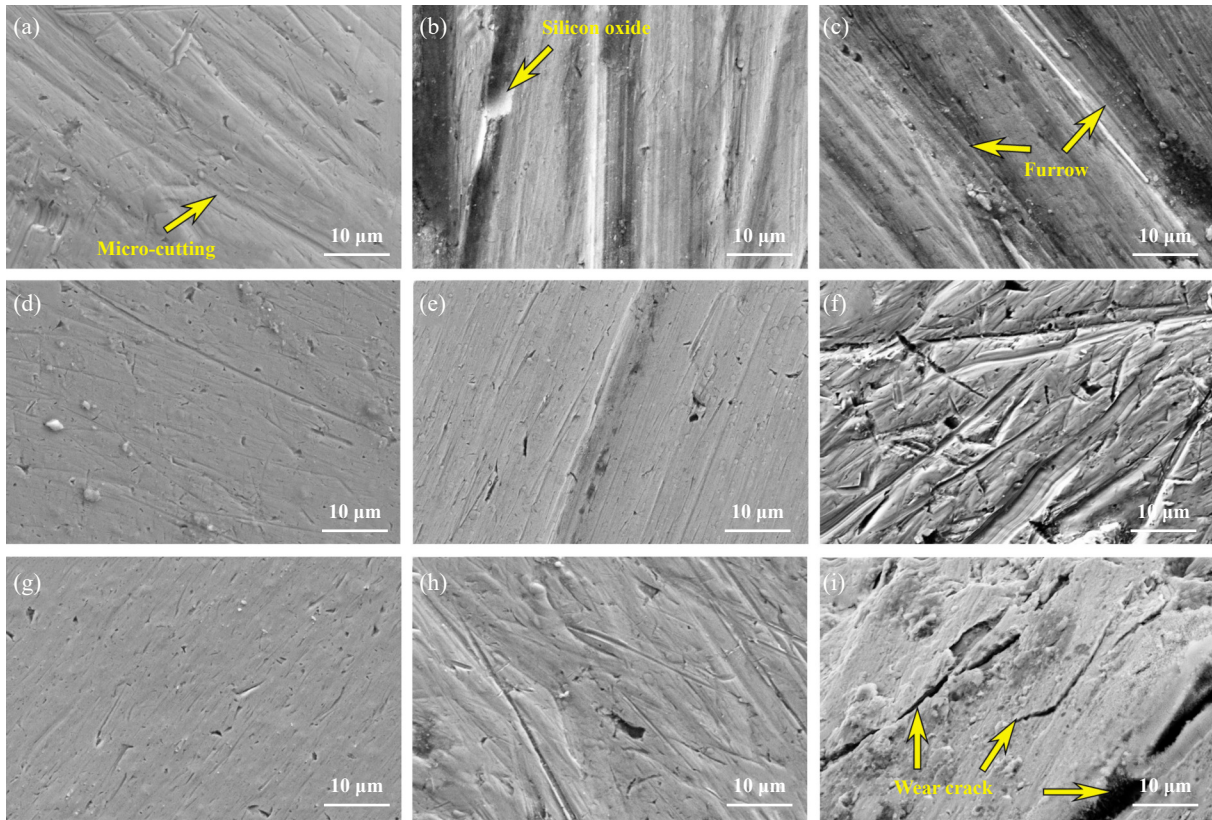


Fig. 4 SEM micrographs of worn surface morphology of experimental steels with different hardness after grinding with granite: (a) C1-1 kN; (b) C1-3 kN; (c) C1-5 kN; (d) C3-1 kN; (e) C3-3 kN; (f) C3-5 kN; (g) C5-1 kN; (h) C5-3 kN; (i) C5-5 kN

图4 与花岗岩配副后不同硬度试验钢的磨损表面形貌的SEM照片

应地减小,同时C3钢韧性低于C1钢,因此切削条带在弯曲过程中容易发生断裂。从图5(e~f)可以看出,硬度最高的C5钢磨屑形态与C1和C3钢明显不同,C5钢的磨屑形态呈木屑状,磨屑长度及卷曲程度明显减小。C5钢硬度最高,但是韧性相对较低,在与磨粒相对滑动过程中,磨屑发生较小弯曲后即可发生断裂,从磨损表面脱落。

图6所示为5 kN载荷下不同硬度试验钢与花岗岩磨损后产生的磨屑形貌的SEM照片及合金元素面分布图。从图7(a~b)可以看出,硬度最低的C1钢与花岗岩产生的磨屑呈细小颗粒状,从磨屑的面分布图可以看出,磨屑主要由Fe、Cr、O和Si组成,说明磨屑为氧化铁与二氧化硅的混合物。相比C1钢,硬度较高的C3钢磨屑尺寸明显增加,并且呈不规则块状,尺寸在100 μm左右,如图7(c~d)所示。从块状磨屑的EDS分析可以看出,磨屑主要由Fe和O组成,说明在磨损过程中试验钢发生了氧化,从试验钢磨损表面脱落的氧化铁附着在岩石碎屑上。C5钢的磨屑尺寸更加粗大,大多数块状磨屑的尺寸超过200 μm。从图7(f)中块状磨屑的背散射电子图像可以看出,磨屑并非为单一的金

属或岩石,结合磨屑的元素面分布图可以看出,磨屑上相对光滑的一面由大量的Fe元素富集,而粗糙的一面则以Si和O元素为主,由此说明磨屑是从花岗岩磨损轨迹表面脱落下来的。在磨损过程中,试验钢与花岗岩发生相对滑动,从试验钢磨损表面脱落的金属附着在磨损轨迹上,在较高磨损载荷下,与试验钢接触的花岗岩在摩擦力作用下被拉断,进而脱落成磨损碎片,因此出现了如图7(f)所示的平整面富含Fe元素,粗糙面富含O和Si元素的磨屑形貌。

### 2.3 磨损亚表面形貌及硬度

图7所示为不同硬度试验钢与砂岩磨损后磨损亚表面的微观组织形貌照片。从图7中可以看出,各试验钢的磨损亚表面均没有出现明显的塑性变形,由此说明试验钢的硬度足够高,具有良好的抗变形能力。与C1钢相比,硬度最高的C5试验钢磨损亚表面非常平整。从图7(a)的局部放大图可以看出,C1钢磨损亚表面的破坏层厚度在2.5 μm左右。图8所示为C1钢磨损亚表面的合金元素面分布图,从图8中可以看出,C1钢磨损表面富集较多的Si和O元素,而磨损亚表面合金元

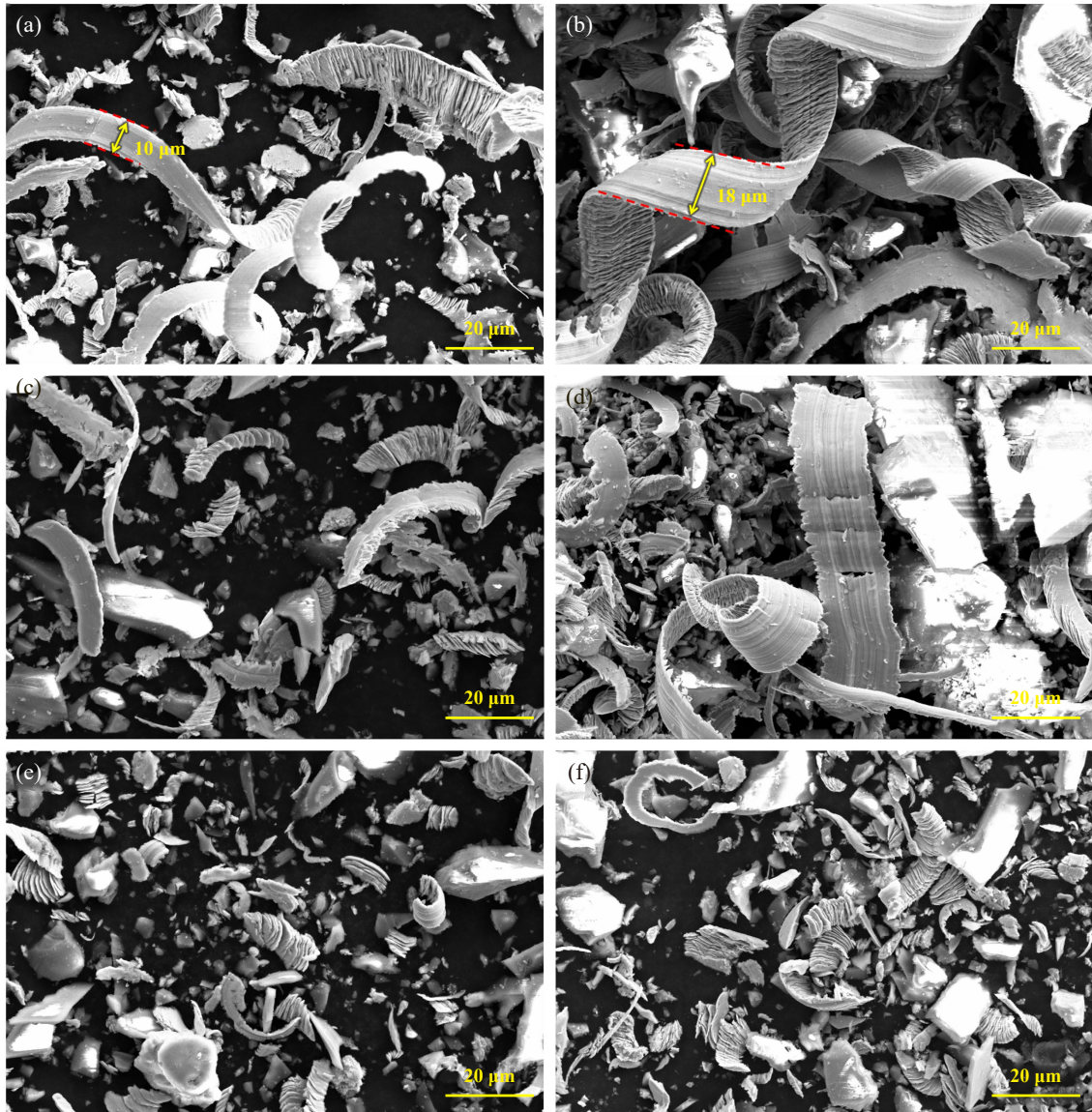


Fig. 5 SEM micrographs of wear debris produced by the grinding of different test steels and sandstone:  
(a) C1-1kN; (b) C1-5kN; (c) C3-1kN; (d) C3-5kN; (e) C5-1kN; (f) C5-5kN

图5 不同试验钢与砂岩磨损后产生的磨屑形貌的SEM照片

素以Fe和Cr为主,说明在磨损过程中试验钢亚表面没有发生氧化,只是在磨损表面黏附了1层二氧化硅岩屑.

图9所示为5 kN磨损载荷下,C1、C3和C5试验钢与砂岩磨损后磨损亚表面的微观组织形貌的SEM照片及合金元素面分布图.从图9(a)可以看出,C1钢磨损亚表面沿磨损方向发生了较为严重的塑性变形,从变形层的合金元素面分布图可以判断出,C1钢磨损面发生了氧化,氧化层的深度在5  $\mu\text{m}$ 左右,氧化层裹挟着细小的富Cr碳化物一起沿磨损方向塑性流动.从图9(b)可以看出,C3钢磨损亚表面没有发生明显的塑性变形,在C3钢磨损表面可以发现1层厚度3  $\mu\text{m}$ 左右的铁氧化层.由于在对磨损亚表面进行SEM观察前,用硝

酸酒精溶剂对试验钢进行了腐蚀,因此在氧化层与基体间腐蚀出1条缝隙.有文献报道,试验钢磨损面上的铁氧化层具有润滑作用,有助于减小磨损失重<sup>[24]</sup>,这也许是5 kN载荷下,C3钢耐磨性最佳的原因之一.C5钢磨损亚表面形貌照片如图9(c)所示,与C1和C3钢不同的是,C5钢磨损亚表面出现了较大的裂纹,这与图4(i)中C5钢磨损表面的裂纹对应,磨屑在摩擦力作用下嵌入到试验钢的裂纹中,加剧了试验钢磨损面的断裂.

图10所示为各试验钢与花岗岩磨损后,磨损亚表面的硬度值.从图10中可以看出,各试验钢磨损亚表面的硬度值并没有随着测试深度的增加单调增加或减小.结合磨损亚表面的微观组织形貌,可以说明磨



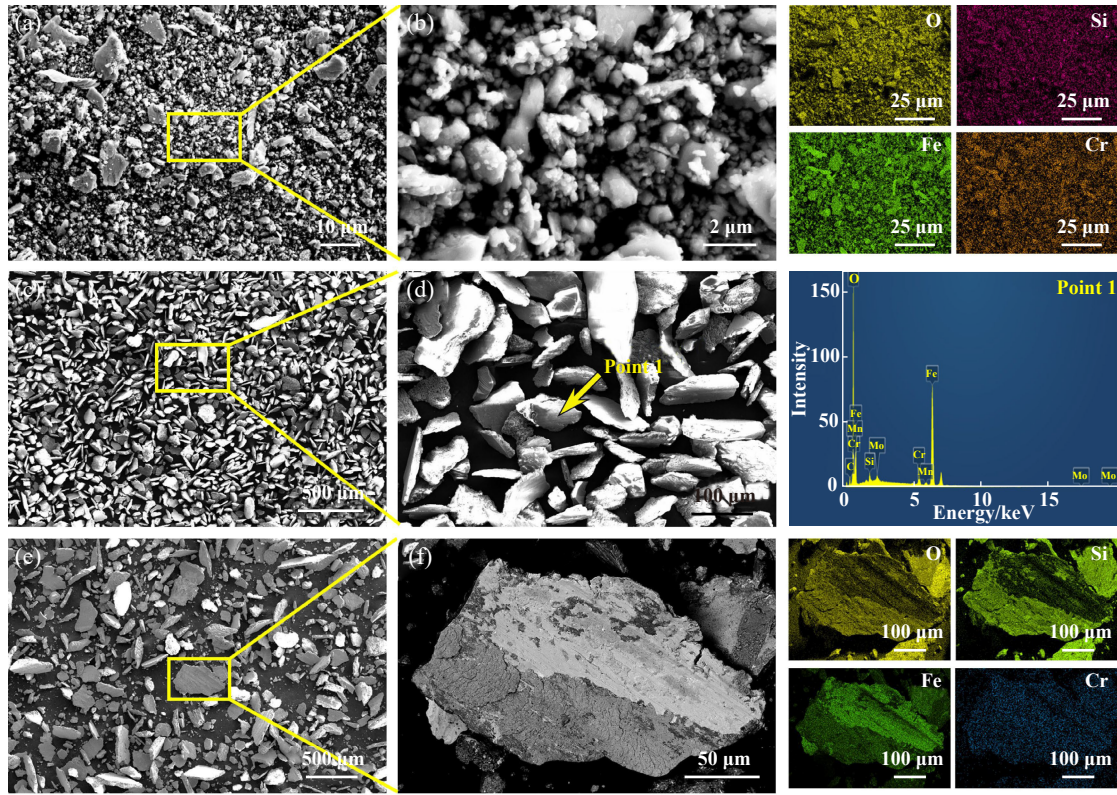


Fig. 6 SEM micrographs and element mappings of wear debris produced by grinding of each test steels and granite under load of 5 kN: (a, b) C1; (c, d) C3; (e, f) C5

图 6 5 kN 载荷下各试验钢与花岗岩对磨后产生的磨屑形貌的 SEM 照片及合金元素面分布图

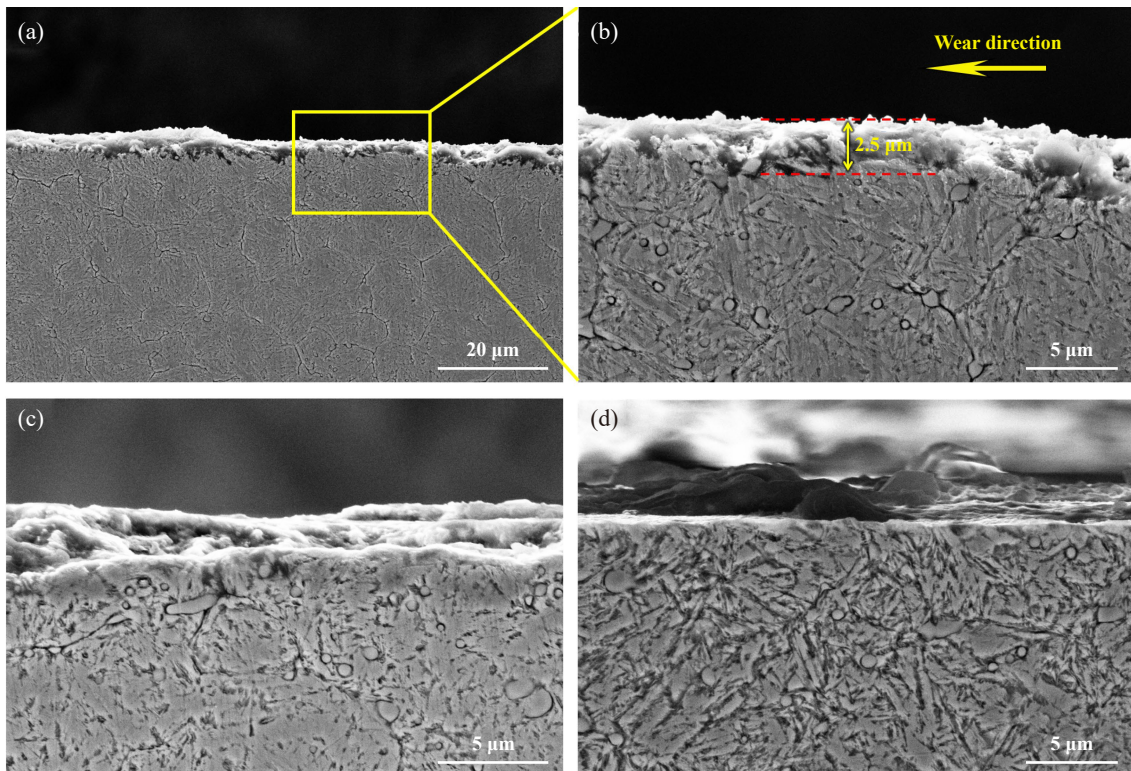


Fig. 7 SEM micrographs of cross-section of each test steels after wear against sandstone: (a, b) C1-5 kN; (c) C3-5 kN; (d) C5-5 kN

图 7 试验钢与砂岩磨损后磨损亚表面断面形貌的 SEM 照片

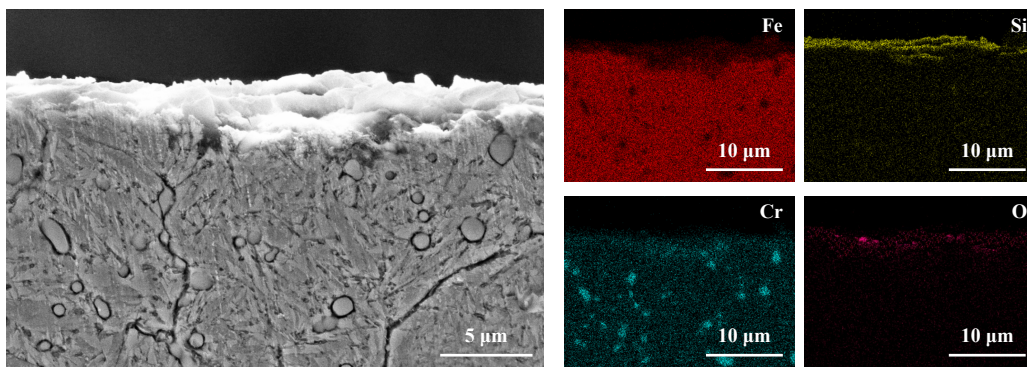


Fig. 8 SEM micrograph and element mapping of cross-section of C1 after wear against sandstone

图8 C1钢磨损亚表面的SEM照片及合金元素面分布图

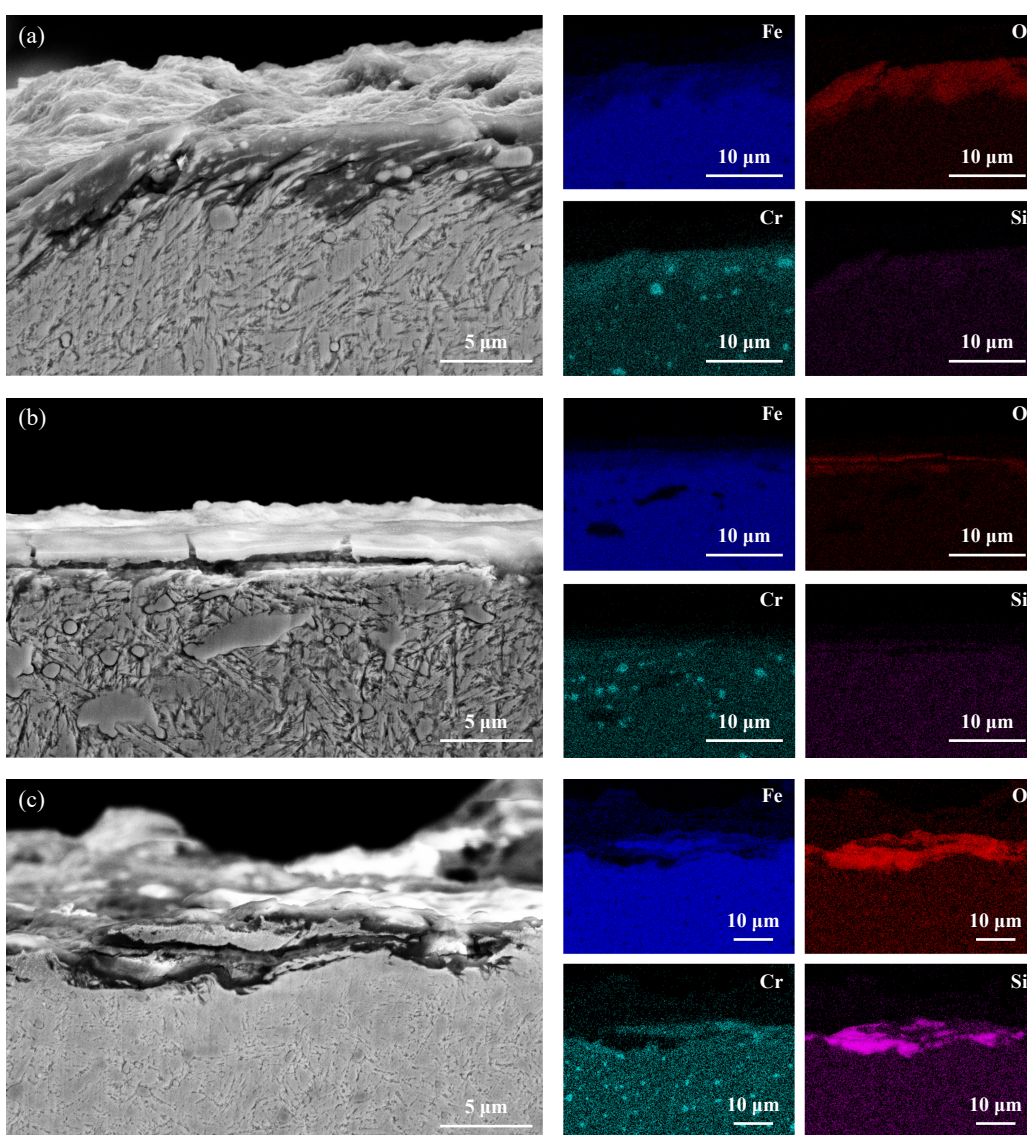


Fig. 9 SEM micrographs and element mappings of cross-section of each tested steels after wear against granite under load of 5 kN: (a, b) C1; (c, d) C3; (e, f) C5

图9 5 kN载荷下各试验钢与花岗岩对磨后磨损亚表面SEM形貌照片及合金元素面分布图

损亚表面未发生明显的微观组织相变或者磨损亚表面相变层厚度过小,使用维氏硬度计未能检测出磨损

亚表面硬度变化.在Yang等<sup>[25]</sup>关于马氏体钢球-盘往复磨损研究中,同样发现马氏体钢磨损亚表面几乎不

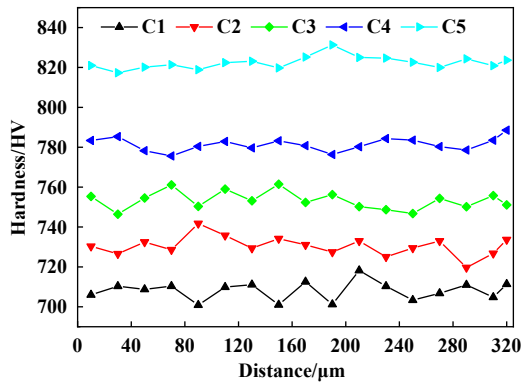


Fig. 10 Subsurface hardness of each experimental steels after against granite under 5 kN load

图 10 5 kN 载荷下与花岗岩相对摩擦后各试验钢磨损亚表面硬度

发生形变,甚至在一些低硬度( $\sim 500$  HV)贝氏体钢的冲击磨损中,磨损变形层的厚度也只有 $2\sim 4\ \mu\text{m}$ <sup>[26]</sup>。

### 3 结论

不同磨损工况下,材料的耐磨性差异较大.本文中设计了具有不同硬度与冲击韧性的TBM刀圈钢,分别研究了砂岩与花岗岩磨损工况下不同性能刀圈的耐磨性及磨损失效机制,为不同岩石工况下TBM刀圈用钢硬度与冲击韧性的选型提供了理论依据.主要研究结论如下:

a. 砂岩工况下,刀圈钢的耐磨性与刀圈自身硬度呈正比.刀圈钢的磨损机制为微观切削,刀圈自身硬度越高,磨损表面的划切深度越小.与砂岩匹配性最佳的刀圈硬度为65.02 HRC,冲击功为6.94 J.

b. 花岗岩工况下,刀圈钢的耐磨性复杂多变.磨损载荷低于3 kN条件下,刀圈钢磨损机制为微观犁削,其耐磨性与自身硬度呈正比,硬度为65.02 HRC,冲击功为6.94 J的刀圈钢耐磨性最佳.磨损载荷为5 kN时,随着刀圈硬度增加,耐磨性先增加后降低,磨损机制由微观犁削向脆性断裂转变,硬度为63.06 HRC,冲击功为8.49 J的刀圈与花岗岩磨损匹配性最佳.

### 参考文献

[1] Hong Kairong, Du Yanliang, Chen Kui, et al. Full-face tunnel boring machines (shields/TBMs) in China: history, achievements, and prospects[J]. Tunnel Construction, 2022, 42(5): 739–756 (in Chinese) [洪开荣, 杜彦良, 陈夔, 等. 中国全断面隧道掘进机发展历程、成就及展望[J]. 隧道建设(中英文), 2022, 42(5): 739–756]. doi: 10.3973/j.issn.2096-4498.2022.05.001.

[2] Qin Haiyang, Liu Houquan, Zhou Hui, et al. Development and prospect of hard rock boring machine in China[J]. Road Machinery

& Construction Mechanization, 2017, 34(2): 19–25 (in Chinese) [秦海洋, 刘厚全, 周慧, 等. 硬岩掘进机在中国的发展与展望[J]. 筑路机械与施工机械化, 2017, 34(2): 19–25].

[3] Duan Wenjun, Zhang Mengqi, Gou Bin, et al. Influence of cross-section profile on wear behavior of TBM cutters in hard rock stratum[J]. Tribology, 2023, 43(7): 738–749 (in Chinese) [段文军, 张蒙祺, 勾斌, 等. 刃形对硬岩地层中TBM滚刀磨损行为的影响研究[J]. 摩擦学学报, 2023, 43(7): 738–749]. doi: 10.16078/j.tribology.2022102.

[4] Ren Dongjie, Shen Shuilong, Arulrajah A, et al. Prediction model of TBM disc cutter wear during tunnelling in heterogeneous ground[J]. Rock Mechanics and Rock Engineering, 2018, 51(11): 3599–3611. doi: 10.1007/s00603-018-1549-3.

[5] Karami M, Zare S, Rostami J. Introducing an empirical model for prediction of disc cutter life for TBM application in jointed rocks: case study, Kerman water conveyance tunnel[J]. Bulletin of Engineering Geology and the Environment, 2021, 80(5): 3853–3870. doi: 10.1007/s10064-021-02166-w.

[6] Yan Hong, Chen Lei, Ruan Xianming. Tempering process of  $5\text{Cr}_5\text{MoSiV1}$  steel for shield tools[J]. Transactions of Materials and Heat Treatment, 2013, 34(S1): 50–55 (in Chinese) [闫洪, 陈磊, 阮先明. 盾构刀具用 $5\text{Cr}_5\text{MoSiV1}$ 钢的回火工艺[J]. 材料热处理学报, 2013, 34(S1): 50–55]. doi: 10.13289/j.issn.1009-6264.2013.s1.013.

[7] Yan Hong, Chen Lei, Ruan Xianming, et al. Quenched microstructure of  $5\text{Cr}_5\text{MoSiV1}$  steel for shield tools[J]. Heat Treatment of Metals, 2013, 38(6): 76–79 (in Chinese) [闫洪, 陈磊, 阮先明, 等. 盾构刀具用 $5\text{Cr}_5\text{MoSiV1}$ 钢淬火火组织[J]. 金属热处理, 2013, 38(6): 76–79]. doi: 10.13251/j.issn.0254-6051.2013.06.031.

[8] Yan Hong, Ruan Xianming, Chen Lei, et al. Study on quenched mechanical properties of  $5\text{Cr}_5\text{MoSiV1}$  steel for shield tools[J]. Hot Working Technology, 2013, 42(10): 191–193, 197 (in Chinese) [闫洪, 阮先明, 陈磊, 等. 盾构刀具用 $5\text{Cr}_5\text{MoSiV1}$ 钢淬火力学性能研究[J]. 热加工工艺, 2013, 42(10): 191–193, 197]. doi: 10.14158/j.cnki.1001-3814.2013.10.055.

[9] Chen Lei. Study on heat treatment characteristics of  $5\text{Cr}_5\text{MoSiV1}$  steel for TBM hob cutter ring[D]. Nanchang: Nanchang University, 2012 (in Chinese) [陈磊. TBM滚刀刀圈用 $5\text{Cr}_5\text{MoSiV1}$ 钢的热处理特性研究[D]. 南昌: 南昌大学, 2012].

[10] Zhang Mengqi. Test and analysis of mechanical properties of TBM tool materials[D]. Changchun: Jilin University, 2018 (in Chinese) [张孟琦. TBM刀具材料力学性能测试分析[D]. 长春: 吉林大学, 2018].

[11] Zhao Zhengyang. Development of high quality disc hob cutter ring for TBM[D]. Qinhuangdao: Yanshan University, 2016 (in Chinese) [赵正阳. 高品质TBM用盘形滚刀刀圈研制[D]. 秦皇岛: 燕山大学, 2016].

[12] Jia Lianhui, Shang Yong, Long Weimin, et al. Effect of alloy composition of materials for TBM cutter rings on microstructure and wear resistance[J]. Journal of Central South University (Science and

- Technology), 2020, 51(10): 2730–2738 (in Chinese) [贾连辉, 尚勇, 龙伟民, 等. TBM滚刀刀圈材料合金成分对组织和耐磨性能的影响[J]. 中南大学学报(自然科学版), 2020, 51(10): 2730–2738]. doi: [10.11817/j.issn.1672-7207.2020.10.005](https://doi.org/10.11817/j.issn.1672-7207.2020.10.005).
- [13] Xia Yimin, Zhou Ming, Mao Qingsong, et al. Wear characteristics of TBM disc-cutter ring under different rock characteristics[J]. Journal of Harbin Engineering University, 2017, 38(9): 1456–1460 (in Chinese) [夏毅敏, 周明, 毛晴松, 等. 不同岩石特性下TBM滚刀刀圈磨损性能[J]. 哈尔滨工程大学学报, 2017, 38(9): 1456–1460]. doi: [10.11990/jheu.201607083](https://doi.org/10.11990/jheu.201607083).
- [14] Xia Yimin, Mao Qingsong, Zhu Zongming, et al. Matching behavior of hardness of TBM cutter ring and rock[J]. Tribology, 2016, 36(3): 304–309 (in Chinese) [夏毅敏, 毛晴松, 朱宗铭, 等. TBM滚刀刀圈硬度与岩石匹配性能试验[J]. 摩擦学学报, 2016, 36(3): 304–309]. doi: [10.16078/j.tribology.2016.03.006](https://doi.org/10.16078/j.tribology.2016.03.006).
- [15] Fu Jie, Zeng Guiying, Zhang Hao, et al. Experimental investigation on wear behaviors of TBM disc cutter ring with different cooling methods[J]. Engineering Failure Analysis, 2022, 134: 106076. doi: [10.1016/j.engfailanal.2022.106076](https://doi.org/10.1016/j.engfailanal.2022.106076).
- [16] Zhang Xuhui, Lin Laikuang, Xia Yimin, et al. Experimental study on wear of TBM disc cutter rings with different kinds of hardness[J]. Tunnelling and Underground Space Technology, 2018, 82: 346–357. doi: [10.1016/j.tust.2018.08.050](https://doi.org/10.1016/j.tust.2018.08.050).
- [17] Qiu Han, Li Jie, Tu Xiaohui, et al. Effect of *in situ* autogenic TiC on abrasive wear properties of a low alloy martensitic steel[J]. Tribology, 2021, 41(3): 357–364 (in Chinese) [邱涵, 李杰, 涂小慧, 等. 原位自生TiC对低合金马氏体钢磨料磨损性能的影响[J]. 摩擦学学报, 2021, 41(3): 357–364]. doi: [10.16078/j.tribology.2020159](https://doi.org/10.16078/j.tribology.2020159).
- [18] Jiang Jinzhe, Liu Yue, Liu Chunming. Effect of forging ratio on the microstructure, mechanical properties and abrasive wear behavior of a new C-Cr-Mo-V martensitic steel[J]. Journal of Materials Research and Technology, 2022, 19: 4076–4091. doi: [10.1016/j.jmrt.2022.06.069](https://doi.org/10.1016/j.jmrt.2022.06.069).
- [19] Jiang Jinzhe, Liu Yue, Liu Chunming. Effect of tempering temperature on the microstructure, mechanical properties and abrasive wear behavior of a new C-Cr-Mo-V alloy steel used in TBM cutter ring[J]. Journal of Materials Research and Technology, 2022, 20: 195–209. doi: [10.1016/j.jmrt.2022.06.156](https://doi.org/10.1016/j.jmrt.2022.06.156).
- [20] Du Kun, Yang Chengzhi, Su Rui, et al. Failure properties of cubic granite, marble, and sandstone specimens under true triaxial stress[J]. International Journal of Rock Mechanics and Mining Sciences, 2020, 130: 104309. doi: [10.1016/j.ijrmms.2020.104309](https://doi.org/10.1016/j.ijrmms.2020.104309).
- [21] Saha G, Valtonen K, Saastamoinen A, et al. Impact-abrasive and abrasive wear behavior of low carbon steels with a range of hardness-toughness properties[J]. Wear, 2020, 450–451: 203263. doi: [10.1016/j.wear.2020.203263](https://doi.org/10.1016/j.wear.2020.203263).
- [22] Ramadas H, Sarkar S, Nath A K. Three-body dry abrasive wear properties of 15-5 precipitation hardening stainless steel produced by laser powder bed fusion process[J]. Wear, 2021, 470–471: 203623. doi: [10.1016/j.wear.2021.203623](https://doi.org/10.1016/j.wear.2021.203623).
- [23] Liu Hailong, Qu Chuanyong, Qin Qinghua. Experimental investigation on skimming wear mechanism between TBM cutter ring and rock[J]. Journal of Experimental Mechanics, 2015, 30(3): 289–298 (in Chinese) [刘海龙, 曲传咏, 秦庆华. TBM滚刀刀圈与岩石的滑动磨损试验研究[J]. 试验力学, 2015, 30(3): 289–298]. doi: [10.7520/1001-4888-14-167](https://doi.org/10.7520/1001-4888-14-167).
- [24] Wang Feng, Qian Dongsheng, Hua Lin, et al. The effect of prior cold rolling on the carbide dissolution, precipitation and dry wear behaviors of M50 bearing steel[J]. Tribology International, 2019, 132: 253–264. doi: [10.1016/j.triboint.2018.12.031](https://doi.org/10.1016/j.triboint.2018.12.031).
- [25] Yang Liqi, Xue Weihai, Gao Siyang, et al. Study on sliding friction and wear behavior of M50 bearing steel with rare earth addition[J]. Tribology International, 2022, 174: 107725. doi: [10.1016/j.triboint.2022.107725](https://doi.org/10.1016/j.triboint.2022.107725).
- [26] Zhang P, Chen J X, Li J, et al. Microstructure evolution mechanism of carbides-free bainite steel during impact abrasive wear[J]. Wear, 2021, 486–487: 204074. doi: [10.1016/j.wear.2021.204074](https://doi.org/10.1016/j.wear.2021.204074).